Inorganic Chemistry

Article

pubs.acs.org/IC

Cubane-Type Cu^{II}_4 and $Mn^{II}_2Mn^{III}_2$ Complexes Based on Pyridoxine: A Versatile Ligand for Metal Assembling

Nadia Marino,[†] Donatella Armentano,*[,†] Teresa F. Mastropietro,[†] Miguel Julve,[‡] Giovanni De Munno,[†] and José Martínez-Lillo*[,†,‡]

[†]Dipartimento di Chimica e Tecnologie Chimiche, Università della Calabria, via P. Bucci 14/c, 87030 Arcavacata di Rende, Cosenza, Italy

[‡]Instituto de Ciencia Molecular (ICMol), Universitat de València, c/Catedrático José Beltrán 2, 46980 Paterna, Valencia, Spain

Supporting Information

ABSTRACT: By using Vitamin B_6 in its monodeprotonated pyridoxine form (PN-H) [PN = 3-hydroxy-4,5-bis-(hydroxymethyl)-2-methylpyridine], two tetranuclear compounds of formula $[Mn_4(PN\text{-}H)_4(CH_3CO_2)_3Cl_2]Cl\cdot 2CH_3OH\cdot 2H_2O$ (**1**) and $[Cu_4(PN\text{-}H)_4Cl_2(H_2O)_2]Cl_2$ (**2**) have been synthesized and magneto-structurally characterized. **1** crystallizes in the triclinic system with space group $P\bar{1}$ whereas **2** crystallizes in the orthorhombic system with *Fdd*2 as space group. They exhibit $Mn^{II}_2Mn^{III}_2$ (**1**) and Cu^{II}_4 (**2**) cubane cores containing four monodeprotonated pyridoxine groups simultaneously acting as chelating and bridging ligands (**1** and **2**), three bridging acetate ligands in the *syn-syn* conformation (**1**), and two terminally bound chloride anions (**1** and **2**) plus two coordinated water molecules (**2**). The electroneutrality is achieved by the presence of chloride counterions in both compounds. Tri- [Mn(1) and Mn(3)] and divalent [Mn(2) and Mn(4)] manganese centers coexist in **1**, all being six-coordinate with distorted $Mn(1/3)O_6$ and $Mn(2/4)O_5Cl$ octahedral surroundings, respectively, the equatorial Mn−O bonds being about 0.2 Å shorter at the former ones. The two crystallographically independent copper(II) ions in **2** are five-coordinate in somewhat distorted CuO_5 [Cu(1)] and CuO_4Cl [Cu(2)] square pyramidal geometries. The values of the intracore metal−metal separation cover the ranges 3.144(1)−3.535(1) (**1**) and 2.922(6)−3.376(1) Å (**2**). The magnetic properties of **1** and **2** were investigated in the temperature range 1.9−300 K, and they correspond to an overall antiferromagnetic behavior with susceptibility maxima at 5.0 (**1**) and 65.0 K (**2**). The analysis of the magnetic susceptibility data showed the coexistence of intracore antiferro- and ferromagnetic interactions in the two compounds. Their values compare well with those existing in the literature for the parent systems.

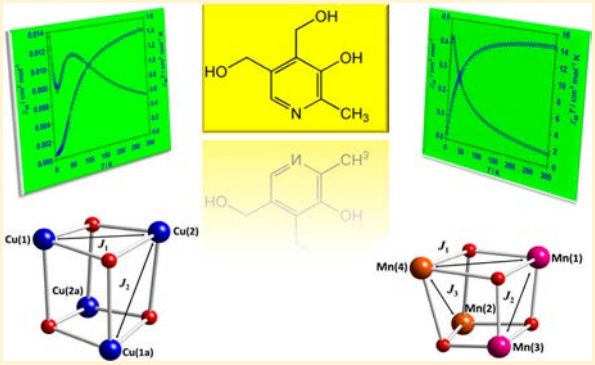

INTRODUCTION

New generations of metal complexes featuring ligands from the biological world are attracting continuous interest in the attempt to develop new materials with tailored architectures and properties.[1−3] The powerful self-assembling features of biomolecules offer the possibility to achieve a fine control over the structure of the material at the nanoscale level. The incorporation of transition metal ions into hierarchically organized structures allows the introduction of addressable functionality and properties.

Countless biomolecules have the ability of binding and/or bridging metal ions exhibiting multiple possible coordination modes.[2,3] Among them, Vitamin B_6 [pyridoxine (PN)] seems to us a particularly attractive ligand for the construction of polynuclear species owing to the presence of several metal coordination sites with different charges and hard/soft character.[4] As far as we know, complexes of Vitamin B_6 have been mainly investigated because of their biological interest.[5] Nevertheless, the presence of aliphatic and aromatic alcohol functionalities on its framework makes this ligand suitable for metal assembling through its multiple alkoxide arms that in principle would be able to adopt both chelating and bridging modes.[6]

It deserves to be pointed out that the question concerning the binding site of the Vitamin B_6 is complicated by the tautomerism possibilities. The pyridoxinate(2-) anion commonly acts as a ligand toward the metal ions via the phenolate-oxygen and the adjacent oxymethyl (see Chart 1).[7] The same coordination mode is exhibited by the monodeprotonated pyridoxine, (N)H-pyridoxinate(1-)[8−11] $[PN\text{-}H]^-$ (hereafter indicated simply as PN-H) and the zwitterionic N-protonated, phenol-deprotonated pyridoxine(0) form.[12−16] Structural evidence for the coordination of pyridoxine through the pyridine-nitrogen are limited to some mononuclear Pd(II)[4,14] complexes and two homometallic Zn(II)[11] and Cu(II)[15] chains, while metal chelation involving the N atom of the pyridine ring has been suggested on the basis of spectroscopic data only.[7]

Received: June 27, 2013
Published: September 27, 2013

   dx.doi.org/10.1021/ic4016355 | *Inorg. Chem.* 2013, 52, 11934−11943

Chart 1

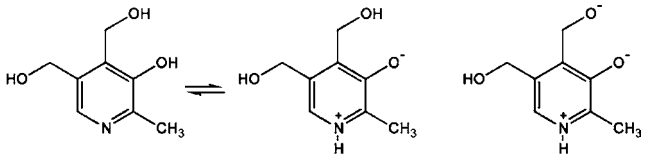

Bearing in mind that the chances to identify new complexes with interesting physical-chemical properties will benefit from the development of new reaction systems with suitable organic ligands, we undertook a systematic study on the reactivity of this biomolecule and first-row transition metal ions.

In this work we report our first results obtained by using Vitamin B_6 as a ligand toward Mn(III) and Cu(II) as metal ions. The synthesis, crystal structures and magnetic properties of two tetranuclear complexes of formula $[Mn_4(PN\text{-}H)_4(CH_3CO_2)_3Cl_2]Cl{\cdot}2CH_3OH{\cdot}2H_2O$ (**1**) and $[Cu_4(PN\text{-}H)_4Cl_2(H_2O)_2]Cl_2$ (**2**) are presented herein. Both compounds display a cubane core, mainly as a consequence of the rare μ_3-pyridoxinate coordination mode.[9] Polynuclear compounds with transition metal ions having a cubane-like framework have received increasing attention as a result of their appealing physicochemical properties and biological relevance.[17,18] Many examples of this special class of discrete polynuclear species have been reported in the literature and extensively reviewed in recent times. In this context, **1** constitutes one more example of tetranuclear mixed-valence $Mn_2^{II}Mn_2^{III}$ compounds,[19−24] and the second reported case exhibiting a single cubane moiety.[25] Concerning compound **2**, a high number of complexes with $Cu^{II}{}_4O_4$ single-cubane motifs have been prepared and magneto-structurally investigated by both experimental and theoretical methods.[26,27] Nevertheless, examples of cubane-like copper(II) framework containing Vitamin B_6 as ligand are limited to one structural type of compound with a "stepped-incomplete-cubane" core.[9]

EXPERIMENTAL SECTION

Materials. Pyridoxine hydrochloride, manganese(III) acetate dihydrate, copper(II) acetate monohydrate, potassium permanganate, manganese(II) acetate monohydrate, 2-propanol, methanol, and *n*-hexane were purchased from commercial sources and used as received. Elemental analyses (C, H, N) were performed on a CE Instruments EA 1110 CHNS analyzer. The values of the Mn:Cl (**1**) and Cu:Cl (**2**) molar ratio [4:3 (**1**) and 1:1 (**2**)] were determined by electron probe X-ray microanalysis at the Servicio Interdepartamental of the University of Valencia.

Synthesis of the Complexes. *Preliminary Note.* Pyridoxine may exist in the neutral, mono-, or dideprotonated form, depending on the value of the pH of the solution. Pyridoxine hydrochloride was used in this work, and no pH adjustment was carried out of the mother solution as the presence alone of copper(II) or manganese(III) acetate, purposely chosen as metal sources, promoted the formation of the monodeprotonated form of pyridoxine. Although a high number of tetranuclear mixed-valence $[Mn^{II}{}_2Mn^{III}{}_2]$ complexes are found in the literature, compound **1** is just the second example exhibiting a single cubane core. Interestingly, the literature complex also features multiple acetate bridges supporting the cubane motif.[25] It seems thus reasonable to suppose that the presence of carboxylate moieties in the synthetic process could play an important role in generating or at least strongly stabilizing the cubane core in this particular II/III mixed-valent state.

$[Mn_4(PN\text{-}H)_4(CH_3CO_2)_3Cl_2]Cl{\cdot}2CH_3OH{\cdot}2H_2O$ (1). A mixture of manganese(III) acetate dihydrate (135.0 mg, 0.5 mmol) and pyridoxine hydrochloride (104.0 mg, 0.5 mmol) in MeOH (5 mL) was stirred during 20 min. The resulting dark brown solution (initial pH value of 5.0) was poured into the bottom of a single test tube, which was filled by a careful addition of *n*-hexane, further closed, and left to diffuse. Polyhedral light brown crystals of **1** appeared in 3−4 days after diffusion at room temperature. Yield: about 65%. Alternatively, **1** was also prepared by using different mixtures of $KMnO_4$ and $Mn(CH_3COO)_2{\cdot}H_2O$, but without any improvement of the quoted yield. Anal. Calcd. for $C_{40}H_{61}N_4O_{22}Cl_3Mn_4$ (**1**): C, 37.65; H, 4.82; N, 4.39. Found: C, 37.42; H, 4.61; N, 4.32%. IR (KBr pellets/cm^{-1}): bands assigned to pyridoxinate ligand appear at 3230s, 3015m, 2919m, 2864m, 1515vs, 1385m, 1350s, 1300w, 1018vs, 840m, 661m, and those associated to the ν_{as}(COO) and ν_s(COO) carboxylate vibrations from the acetate ligand appear at 1563vs and 1420s, respectively.

$[Cu_4(PN\text{-}H)_4Cl_2(H_2O)_2]Cl_2$ (2). Compound **2** was prepared by slow diffusion in an H-shaped tube at room temperature: pyridoxine hydrochloride (41.2 mg, 0.2 mmol) dissolved in water (1 mL) was placed in one arm whereas copper(II) acetate monohydrate (40.0 mg, 0.2 mmol) also dissolved in water (1 mL) was introduced in the other arm. Then, 2-propanol was carefully added in both arms until the H-tube was filled; it was allowed to diffuse at room temperature. X-ray quality green polyhedra of **2** appeared after 2−3 weeks in the bridge of the H-shaped tube. The diffusion was completed in about 1 month. A small amount of a brown solid was formed together with the crystals. It was easily removed and discarded. Yield: about 40−45%. Anal. Calcd. for $C_{32}H_{44}N_4O_{14}Cl_4Cu_4$ (**2**): C, 34.79; H, 4.01; N, 5.07. Found: C, 34.51; H, 3.96; N, 4.91%. IR (KBr pellets/cm^{-1}): bands associated to pyridoxinate ligand appear at 3238s, 3015m, 2915m, 2873m, 1519vs, 1389m, 1365s, 1303w, 1012s, 848m and 658m.

Physical Measurements. Infrared spectra were recorded with a Thermo-Nicolet 6700 FT-IR spectrophotometer as KBr pellets in the 4000−400 cm^{-1} region. Magnetic measurements on polycrystalline samples of **1** and **2** were carried out on a Quantum Design SQUID magnetometer in the temperature range 1.9−300 K and under applied dc magnetic fields of 1 T ($100 \leq T \leq 300$ K) and 100 G ($1.9 \leq T < 100$ K). The magnetic susceptibility data were corrected for the diamagnetic contributions of the constituent atoms (estimated from Pascal's constants) as well as for the sample holder.

X-ray Data Collection and Structure Refinement. Single-crystal X-ray diffraction data of **1** and **2** were collected on a Bruker-Nonius X8APEXII CCD area detector diffractometer using graphite-monochromated Mo−K_α radiation at low temperature [100(2) K], performing generic φ-and ω-scans. Suitable crystals of approximate dimensions 0.03 × 0.06 × 0.08 (**1**) and 0.03 × 0.10 × 0.12 mm^3 (**2**) were selected for data collection. Multiscan absorption corrections were calculated using SADABS.[28]

The structures of **1** and **2** were solved by direct methods using SHELXS and refined against F^2 on all data by full-matrix least-squares with SHELXL-97.[29] All non-hydrogen atoms were refined anisotropically. The hydroxyl oxygen atom [O(3)] in **1**, on one of the four PN-H ligands was found disordered, three sites could be found for it, and their relative occupancies reached values of about 0.47, 0.33, and 0.20 at convergence. Rigid-bond restraints[30] were applied to the four PN-H ligands as well as to the acetate groups in **1** to help stabilize the refinement. The hydrogen atoms on the PN-H ligands at **1** and **2** and those on the acetate groups at **1** were set in calculated positions and refined as riding atoms. In the refinement of the structure of **1**, however, it was not possible to find a reasonable model for the disordered solvent molecules.

The contribution to the diffraction pattern from the two methanol and two water molecules of crystallization, which are located in the channels of the lattice (18.2 % percentage void volume of the unit cell), were subtracted from the observed data by using the SQUEEZE method, as implemented in PLATON.[31] The residual agreement factors for reflections with $I > 2\sigma(I)$ for **1** were $R_1 = 0.0899$ and $wR_2 = 0.2748$ before SQUEEZE whereas they were and $R_1 = 0.0459$ and $wR_2 = 0.1305$ after SQUEEZE. The final formulation of the compound is in agreement with the residual electron density and volume. In the refinement of the structure of **2**, the hydrogen atoms on the water

dx.doi.org/10.1021/ic4016355 | Inorg. Chem. 2013, 52, 11934−11943

molecule O(1w) linked to Cu(1) were located on the ΔF map and refined with restraints, with thermal factors fixed to 1.5 times the U value of O(1w).

The final geometrical calculations and the graphical manipulations were performed using the XP utility within SHELXL[29b] and the DIAMOND software.[32] Crystal data for **1** and **2** are summarized in Table 1. CCDC reference numbers are 945720 (**1**) and 945721 (**2**).

Table 1. Summary of Crystal Data for $[Mn_4(PN\text{-}H)_4(CH_3CO_2)_3Cl_2]Cl\cdot 2CH_3OH\cdot 2H_2O$ (1) and $[Cu_4(PN\text{-}H)_4Cl_2(H_2O)_2]Cl_2$ (2)

	1	2
formula	$C_{40}H_{61}Cl_3Mn_4N_4O_{22}$	$C_{16}H_{22}Cl_2Cu_2N_2O_7$
M_r	1276.04	1104.67
crystal system	Triclinic	Orthorhombic
space group	$P\bar{1}$	$Fdd2$
a/Å	11.6914(5)	31.315(2)
b/Å	11.8134(5)	13.7554(8)
c/Å	20.2545(8)	17.9847(8)
α/deg	97.992(2)	90
β/deg	102.438(2)	90
γ/deg	90.994(2)	90
V/Å^3	2702.0(2)	7747.0(8)
Z	2	8
D_c/g cm^{-3}	1.568	1.894
T/K	100(2)	100(2)
$F(000)$	1312	4480
$\mu(Mo\text{-}K\alpha)$/mm^{-1}	1.140	2.516
refl. collected	58864	36901
refl. indep. (R_{int})	10193 (0.0474)	3728 (0.0701)
refl. obs. [$I > 2\sigma(I)$]	7851	3198
$R_1{}^a$ [$I > 2\sigma(I)$] (all)	0.0459 (0.0649)	0.0343 (0.0453)
$wR_2{}^b$ [$I > 2\sigma(I)$] (all)	0.1305 (0.1375)	0.0805 (0.0854)
goodness-of-fit on F^2	1.073	1.055
abs. struct. param.		0.31(1)
$\Delta\rho_{max,\ min}$/e Å^{-3}	1.060, −0.620	0.543, −0.549

$^aR_1 = \sum(|F_o| - |F_c|)/\sum|F_o|$. $^bwR_2 = \{\sum[w(F_o^2 - F_c^2)^2]/\sum[w(F_o^2)^2]\}^{1/2}$ and $w = 1/[\sigma^2(F_o^2) + (mP)^2 + nP]$ with $P = (F_o^2 + 2F_c^2)/3$, $m = 0.0738$ (**1**), 0.0502 (**2**), and $n = 2.6314$ (**1**), 3.8363 (**2**).

RESULTS AND DISCUSSION

Description of the Crystal Structure of $[Mn_4(PN\text{-}H)_4(CH_3CO_2)_3Cl_2]Cl\cdot 2CH_3OH\cdot 2H_2O$ (1). Compound **1** crystallizes in the triclinic space group $P\bar{1}$, with the whole molecule in the asymmetric unit. Its structure consists of monocationic, tetranuclear $[Mn^{II}_2Mn^{III}_2(PN\text{-}H)_4(CH_3CO_2)_3Cl_2]^+$ units exhibiting a cubane-type arrangement, uncoordinated chloride anions, and crystallization solvent molecules.

The oxidation state of the four crystallographically independent metal centers in the cubane moiety in **1** could be easily assigned on the basis of a crystallographic bond distance analysis (see Table 2). Bond valence sum (BVS) calculations[33] (Table 3) confirmed the Mn(1)−Mn(3) and Mn(2)−Mn(4) pairs as the two Mn(III) and the two Mn(II) centers, respectively. The overall tetranuclear cation in **1** can be divided into two subunits, each containing one Mn(III) and one Mn(II) centers [Mn(1)−Mn(2) and Mn(3)−Mn(4), respectively] plus two PN-H ligands. As shown in Figure 1, both PN-H ligands in each subunit chelate the Mn(III) center [either Mn(1) or Mn(3)] through the phenolate and the adjacent oxymethyl-oxygen atoms, in a *cis* fashion (meaning that both ligands show the same orientation with respect to each other). The two oxymethyl-oxygen atoms are further directed toward the Mn(II) center [either Mn(2) or Mn(4)], in a bidentate manner. Each dinuclear unit is also supported by an acetate bridge in the *syn-syn* conformation.

The tetranuclear, cubane-like arrangement arises from the interaction between these two subunits via four direct Mn−O bonds, all involving the oxymethyl-oxygen atom on each ligand [Mn(1)−O(23), Mn(2)−O(22), Mn(3)−O(2), Mn(4)−O(21)], which exhibits an overall μ_3-bridging mode. A third acetate group with the *syn-syn* conformation is also present that supports the cubane moiety by linking the two Mn(II) centers, one on each subunit [Mn(2)−O(8)−C(18)−O(9)−Mn(4)] (see Figure 2). A coordinated chloride anion completes the coordination sphere of the Mn(II) ions. Each Mn(III) ion [Mn(1) and Mn(3)] shows a typical axially elongated octahedral geometry because of the Jahn−Teller effect. The oxygen atoms of the two chelating PN-H ligands in each subunit fill the equatorial plane of either Mn(1) or Mn(3), with short Mn−O distances in the range 1.877(3)−1.957(2) Å; the axial positions are occupied by either an oxygen atom from the bridging acetate ion in the same subunit (Figure 1) or an oxymethyl-oxygen atom from the other subunit (Figure 2), with long Mn−O distances in the range 2.158(3)−2.378(3) Å.

Each Mn(II) ion [Mn(2), Mn(4)] also shows a distorted octahedral environment, the shortest Mn−O bonds being those involving the acetate groups, and the longest metal−ligand bond being that with the chloride ion (see Table 2). The two bis-chelated $[Mn^{III}(PN\text{-}H)_2]$ fragments on each subunit in the cubane moiety are rotated about 90° with respect to each other (see Figure 2c). As a result, only two of the four PN-H ligands face to each other, while the other two are placed on opposite sides of the cubane core. The two facing PN-H weakly interact via a C−H···π pathway involving the pyridine moiety at one ligand and the methyl group from the other [C−H···π_{centr} distances and CH···π_{centr}···N angles in the ranges 2.7−2.9 Å and 73−80°, respectively].

The crystal packing in **1** is dictated by hydrogen bonds involving both the coordinated and the uncoordinated chloride ions as well as the bridging acetate ions, the protonated pyridinic nitrogen, and the uncoordinated hydroxymethyl group of the PN-H ligands. Details are given in the Supporting Information, Figures S1 and S2 and Table S1.

Description of the Crystal Structure of $[Cu_4(PN\text{-}H)_4Cl_2(H_2O)_2]Cl_2$ (2). Compound **2** crystallizes in the orthorhombic space group $Fdd2$. Its structure consists of centrosymmetric $[Cu_4(PN\text{-}H)_4Cl_2(H_2O)_2]^{2+}$ cubane-type cationic units (Figure 3) and noncoordinated chloride anions. The asymmetric unit contains a pyridoxinato-bridged dicopper(II) motif having two crystallographically independent copper(II) ions [Cu(1) and Cu(2)] and two PN-H ligands (Figure 3a). Each Cu(II) ion is five-coordinate, in a rather distorted square pyramidal environment. Both ligands chelate one of the two copper centers through the phenolate and the adjacent oxymethyl-oxygen atoms, the latter one further acting as donor toward the other copper(II) ion, [Cu−O bond distances and Cu−O−Cu angles in the range 1.925(3)−1.984(4) Å and 96.70(17)−96.86(15)°, respectively]. A water molecule [at Cu(1)] and a chloride anion [at Cu(2)] complete the two basal planes. The cubane-type arrangement results from the self-assembling of two of these dinuclear subunits, via four long Cu−O bonds with Cu−O−Cu angles close to 100° [values in the range 2.408(3)−2.446(3) Å and 96.67(13)−101.00(12)°, respectively] (Figure 3b). The oxymethyl-oxygen atom on both

dx.doi.org/10.1021/ic4016355 | Inorg. Chem. 2013, 52, 11934−11943

Table 2. Selected Geometric Parameters[a] for 1

		Bond Distances	
Mn(1)−O(1)	1.879(2)	Mn(3)−O(12)	1.877(3)
Mn(1)−O(2)	1.942(2)	Mn(3)−O(13)	1.891(3)
Mn(1)−O(11)	1.891(2)	Mn(3)−O(21)	2.341(2)
Mn(1)−O(21)	1.925(2)	Mn(3)−O(22)	1.957(2)
Mn(1)−O(23)	2.378(3)	Mn(3)−O(23)	1.921(2)
Mn(1)−O(4)	2.206(3)	Mn(3)−O(6)	2.158(3)
Mn(2)−O(2)	2.346(2)	Mn(4)−O(2)	2.290(3)
Mn(2)−O(21)	2.225(2)	Mn(4)−O(22)	2.285(2)
Mn(2)−O(22)	2.226(3)	Mn(4)−O(23)	2.242(2)
Mn(2)−O(5)	2.156(3)	Mn(4)−Cl(2)	2.4185(11)
Mn(2)−Cl(1)	2.4220(11)	Mn(4)−O(7)	2.178(3)
Mn(2)−O(8)	2.109(3)	Mn(4)−O(9)	2.131(3)
		Metal−Metal Distances	
Mn(1)···Mn(2)	3.1632(7)	Mn(2)···Mn(4)	3.3226(8)
Mn(1)···Mn(3)	3.3483(8)	Mn(2)···Mn(3)	3.4635(8)
Mn(1)···Mn(4)	3.5347(8)	Mn(3)···Mn(4)	3.1441(7)
		Bond Angles	
O(1)−Mn(1)−O(2)	91.17(10)	O(12)−Mn(3)−O(13)	94.09(10)
O(1)−Mn(1)−O(11)	88.37(10)	O(12)−Mn(3)−O(21)	90.77(11)
O(1)−Mn(1)−O(21)	171.56(11)	O(12)−Mn(3)−O(22)	171.61(12)
O(1)−Mn(1)−O(23)	95.19(10)	O(12)−Mn(3)−O(23)	94.62(11)
O(1)−Mn(1)−O(4)	98.89(11)	O(12)−Mn(3)−O(6)	100.11(10)
O(2)−Mn(1)−O(11)	174.22(11)	O(13)−Mn(3)−O(21)	176.21(11)
O(2)−Mn(1)−O(21)	88.70(10)	O(13)−Mn(3)−O(22)	90.54(11)
O(2)−Mn(1)−O(23)	75.28(9)	O(13)−Mn(3)−O(23)	93.66(11)
O(2)−Mn(1)−O(4)	89.72(10)	O(13)−Mn(3)−O(6)	76.12(9)
O(11)−Mn(1)−O(21)	90.92(10)	O(21)−Mn(3)−O(22)	77.59(10)
O(11)−Mn(1)−O(23)	99.02(10)	O(21)−Mn(3)−O(23)	163.71(9)
O(11)−Mn(1)−O(4)	96.04(10)	O(21)−Mn(3)−O(6)	88.30(10)
O(21)−Mn(1)−O(4)	89.55(10)	O(22)−Mn(3)−O(23)	90.02(10)
O(21)−Mn(1)−O(23)	76.61(9)	O(22)−Mn(3)−O(6)	93.73(11)
O(23)−Mn(1)−O(4)	159.62(9)	O(23)−Mn(3)−O(6)	94.09(10)
O(2)−Mn(2)−O(21)	72.45(8)	O(2)−Mn(4)−O(22)	82.42(9)
O(2)−Mn(2)−O(22)	82.43(9)	O(2)−Mn(4)−O(23)	71.90(9)
O(2)−Mn(2)−Cl(1)	176.64(7)	O(2)−Mn(4)−O(7)	158.83(9)
O(2)−Mn(2)−O(5)	86.28(9)	O(2)−Mn(4)−O(9)	90.96(10)
O(2)−Mn(2)−O(8)	86.70(9)	O(2)−Mn(4)−Cl(2)	96.85(7)
O(21)−Mn(2)−O(22)	73.61(9)	O(22)−Mn(4)−O(23)	73.27(9)
O(21)−Mn(2)−Cl(1)	104.52(7)	O(22)−Mn(4)−O(7)	86.53(9)
O(21)−Mn(2)−O(5)	91.39(9)	O(22)−Mn(4)−O(9)	87.72(10)
O(21)−Mn(2)−O(8)	156.86(10)	O(22)−Mn(4)−Cl(2)	176.92(7)
O(22)−Mn(2)−Cl(1)	98.18(7)	O(23)−Mn(4)−O(7)	87.65(9)
O(22)−Mn(2)−O(5)	163.38(9)	O(23)−Mn(4)−O(9)	155.64(10)
O(22)−Mn(2)−O(8)	94.20(10)	O(23)−Mn(4)−Cl(2)	103.66(7)
O(5)−Mn(2)−Cl(1)	92.40(8)	O(7)−Mn(4)−O(9)	106.65(11)
O(5)−Mn(2)−O(8)	97.30(10)	O(7)−Mn(4)−Cl(2)	93.21(8)
O(8)−Mn(2)−Cl(1)	96.53(8)	O(9)−Mn(4)−Cl(2)	95.29(8)
Mn(1)−O(2)−Mn(2)	94.59(10)	Mn(2)−O(2)−Mn(4)	91.57(8)
Mn(1)−O(2)−Mn(4)	113.02(11)	Mn(2)−O(21)−Mn(3)	98.62(9)
Mn(1)−O(21)−Mn(2)	99.06(10)	Mn(2)−O(22)−Mn(3)	111.61(11)
Mn(1)−O(21)−Mn(3)	102.99(10)	Mn(2)−O(22)−Mn(4)	94.86(9)
Mn(1)−O(23)−Mn(3)	101.78(11)	Mn(3)−O(22)−Mn(4)	95.35(10)
Mn(1)−O(23)−Mn(4)	99.79(9)	Mn(3)−O(23)−Mn(4)	97.78(10)

[a]Bond distances (Å), metal−metal distances (Å), and bond angles (deg).

PN-H ligands occupies the apical position at the other copper(II) ion, connecting the two dinuclear subunits. The vertexes of the cubane structure are thus alternately occupied by the four metal ions and the oxymethyl groups of four PN-H ligands, each one exhibiting an overall μ_3-bridging mode, as also observed in **1**. Selected bond distances and angles and metal−metal distances within the cubane moiety in **2** are listed in Table 4.

The coordination mode of the PN-H ligands found in both **1** and **2** is unusual, and it was only observed in a stepped cubane-

dx.doi.org/10.1021/ic4016355 | Inorg. Chem. 2013, 52, 11934−11943

Table 3. Bond Valence Sum (BVS) Calculations for the Mn Ions in Compound 1[a]

atom	Mn^{II}	Mn^{III}	Mn^{IV}
Mn(1)	3.5	**3.2**	3.2
Mn(2)	**1.8**	1.6	1.6
Mn(3)	3.4	**3.2**	3.1
Mn(4)	**1.8**	1.7	1.7

[a]The values in bold are the closest ones to the charge for which it is calculated. The oxidation state for each ion is the nearest integer number to the value in bold.

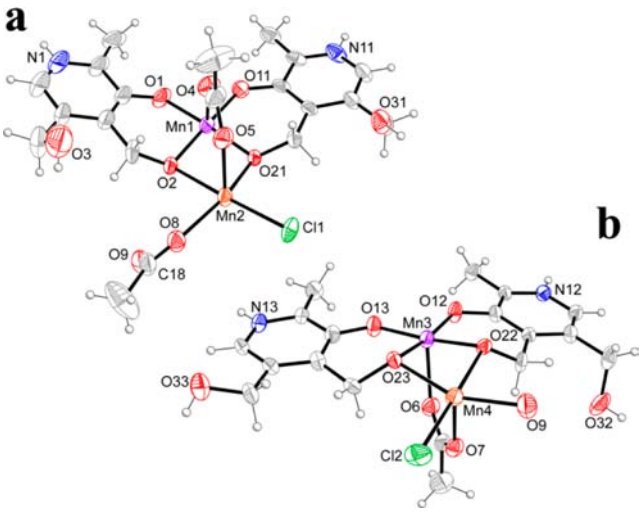

Figure 1. View of the cubane moiety in **1** divided into two subunits for the sake of clarity, showing the atom numbering [only one of the two possible orientations of O(3) is shown]. Thermal ellipsoids are drawn at the 50% probability level. The two depicted subunits interact via four direct Mn−O bonds and an acetate bridge (see Figure 2a). [Note: orange and purple colors refer to Mn^{II} and Mn^{III} ions, respectively].

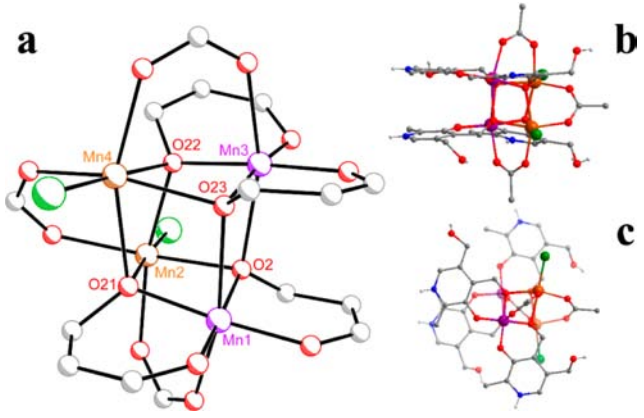

Figure 2. (a) Ball-and-stick representation of the cubane moiety in **1** (only the coordinated oxygen atoms of the PN-H ligands are shown). Side (b) and top (c) views of the complete cubane motifs. [Color code: C, gray; O, red; N, blue; Cl, green; Mn^{II}, orange; Mn^{III}, purple].

like copper(II) complex[9]. Indeed, the Vitamin B_6 in the two copper(II) complexes adopts the bidentate (across the phenolate and oxomethyl group)/monodentate (through the oxomethyl group) coordination mode, as previously observed.[7−11] Nevertheless the further involvement in coordination of the oxymethyl group (μ_3-bridging mode) is crucial toward the formation of the cubane-like moiety observed in **1**

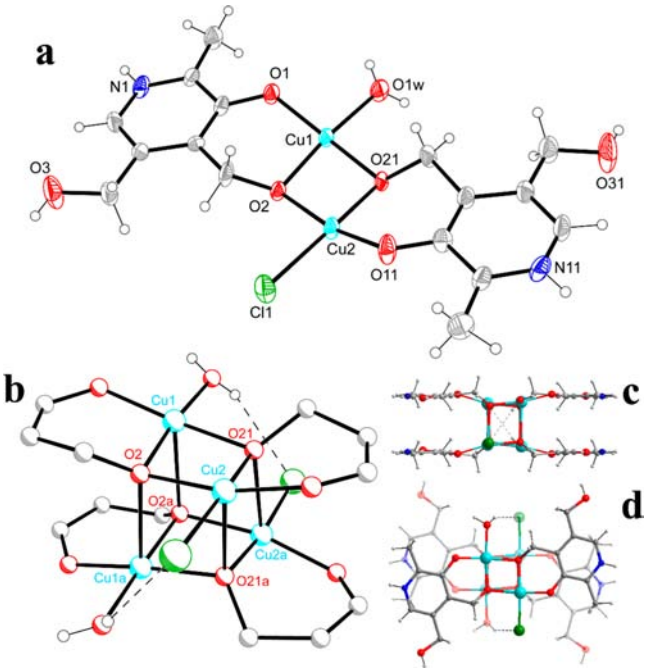

Figure 3. (a) View of the cubane dinuclear subunit in **2** together with the atom numbering. Thermal ellipsoids are drawn at the 50% probability level. (b) Ball-and-stick representation of the cubane-like moiety in **2** (the PN-H ligands are only partially shown for clarity). (c) Side (along the *a* axis) and (d) top (long the *b* axis) views of the complete cubane motif. [The intramolecular O_w-H···Cl hydrogen bonds are indicated by dashed lines].

and **2**. The tetranuclear cores in **1** and **2** being similar are somewhat different because the two PN-H ligands in each [Mn^{II}−Mn^{III}] or [Cu_2^{II}] subunit exhibit a different arrangement. As shown in Figure 4, the two PN-H ligands in **2** are oppositely oriented with respect to each other, each one chelating a single metal ion in a *trans* disposition. On the contrary, the two PN-H ligands at each [Mn^{II}−Mn^{III}] subunit in **1** chelate both the same Mn(III) metal ion in a *cis* arrangement. Focusing on the whole cubane moiety of **2**, one can see that both sets of ligands come offset face-to-face (Figures 3c,d) and interact via a C−H···π pathway similar to that observed in **1**, with CH···π_{centr} distances and CH···π_{centr}···N angles in the ranges 2.96−3.15 Å and 79−84, approximately. Furthermore, a hydrogen bond is established between the coordinated water molecule of one subunit with the coordinated chloride anion of the other subunit (Figure 3).

The coordinated water molecules and chloride anions are also involved in H-bonding interactions, giving rise to a supramolecular step-like 1D motif, running along the crystallographic [1 −1 0] direction.

Further details concerning the crystal packing of **2** are given in the Supporting Information (Figure S3 and Table S2).

Magnetic Properties of 1 and 2. The magnetic properties of **1** in the form of $\chi_M T$ and χ_M versus T plots (χ_M being the magnetic susceptibility per $Mn^{II}_2Mn^{III}_2$ tetranuclear unit) are shown in Figure 5. At room temperature, $\chi_M T$ is equal to 14.50 $cm^3\ mol^{-1}\ K$, a value which is very close to that expected for two Mn(II) ($S_{Mn(II)} = 5/2$) and two Mn(III) ($S_{Mn(III)} = 2$) ions magnetically noninteracting ($\chi_M T$ = 14.75 $cm^3\ mol^{-1}\ K$ with $g_{Mn} = 2.0$). Upon cooling, $\chi_M T$ continuously decreases to reach a minimum value of about 0.025 $cm^3\ mol^{-1}\ K$ at 1.9 K. The χ_M versus T plot exhibits a maximum of the magnetic susceptibility

dx.doi.org/10.1021/ic4016355 | Inorg. Chem. 2013, 52, 11934−11943

Table 4. Selected Geometric Parameters for 2[a,b]

		Bond Distances	
Cu(1)−O(1)	1.896(3)	Cu(2)−O(11)	1.896(4)
Cu(1)−O(2)	1.925(3)	Cu(2)−O(2)	1.984(4)
Cu(1)−O(21)	1.956(4)	Cu(2)−O(21)	1.950(3)
Cu(1)−O(1w)	1.987(3)	Cu(2)−Cl(1)	2.272(1)
Cu(1)−O(2a)	2.446(3)	Cu(2)−O(21a)	2.408(3)
		Metal−Metal Distances	
Cu(1)···Cu(2)	2.9219(6)	Cu(1)···Cu(2a)	3.3235(6)
Cu(1)···Cu(1a)	3.3038(11)	Cu(2)···Cu(2a)	3.3758(11)
		Bond Angles	
O(1)−Cu(1)−O(2)	94.23(15)	O(2)−Cu(2)−O(11)	166.88(15)
O(1)−Cu(1)−O(21)	171.58(16)	O(2)−Cu(2)−O(21)	81.39(13)
O(1)−Cu(1)−O(1w)	90.94(15)	O(2)−Cu(2)−Cl(1)	93.41(9)
O(1)−Cu(1)−O(2a)	105.91(16)	O(2)−Cu(2)−O(21a)	81.95(13)
O(2)−Cu(1)−O(21)	82.77(15)	O(11)−Cu(2)−O(21)	94.08(14)
O(2)−Cu(1)−O(1w)	173.96(17)	O(11)−Cu(2)−Cl(1)	92.21(10)
O(2)−Cu(1)−O(2a)	82.32(11)	O(11)−Cu(2)−O(21a)	109.35(15)
O(21)−Cu(1)−O(1w)	92.50(14)	O(21)−Cu(2)−Cl(1)	172.25(11)
O(21)−Cu(1)−O(2a)	81.55(13)	O(21)−Cu(2)−O(21a)	78.68(12)
O(1w)−Cu(1)−O(2a)	93.31(13)	Cl(1)−Cu(2)−O(21a)	94.96(8)
Cu(1)−O(2)−Cu(2)	96.70(17)	Cu(1)−O(21)−Cu(2)	96.83(15)
Cu(1)−O(2)−Cu(1a)	97.51(11)	Cu(2)−O(2)−Cu(1a)	96.67(13)
Cu(1)−O(21)−Cu(2a)	98.66(14)	Cu(2)−O(21)−Cu(2a)	101.00(12)

[a]Bond distances (Å), metal−metal distances (Å), and bond angles (deg). [b]Symmetry transformation used to generate equivalent atoms: (a) $-x - 1/2, -y + 3/2, z$.

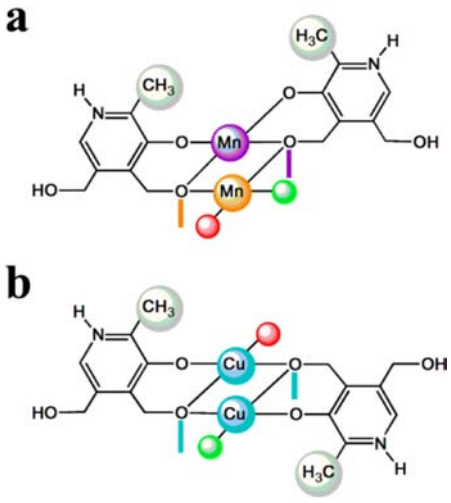

Figure 4. Schematic representation of the overall metal−ligand arrangement in each structural subunit in **1** (a), and **2** (b).

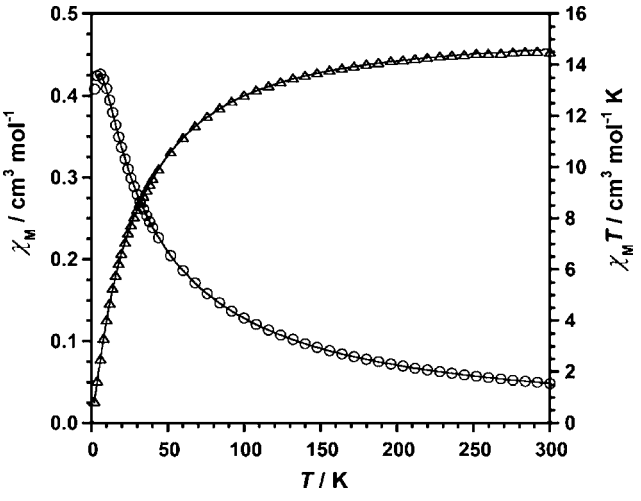

Figure 5. Thermal variation of χ_M (O) and $\chi_M T$ (Δ) for **1**. The solid lines are the best-fit curves (see text).

at 5.0 K. These features are consistent with an overall antiferromagnetic coupling leading to a $S = 0$ ground spin state. Given the nature of the Mn_4O_4 core in **1**, three different magnetic interactions would be involved, corresponding to the Mn^{II}−Mn^{III}, Mn^{III}−Mn^{III}, and Mn^{II}−Mn^{II} pathways and whose magnetic coupling parameters are named J_1, J_2, and J_3, respectively (see Figure 6). Consequently, the magnetic susceptibility data of **1** were treated through the isotropic spin Hamiltonian of eq 1, and the VMPAG package.[34]

$$\hat{H} = -J_1(\hat{S}_1\cdot\hat{S}_2 + \hat{S}_1\cdot\hat{S}_4 + \hat{S}_2\cdot\hat{S}_3 + \hat{S}_3\cdot\hat{S}_4) - J_2(\hat{S}_1\cdot\hat{S}_3) - J_3(\hat{S}_2\cdot\hat{S}_4) \quad (1)$$

Least-squares best-fit parameters for **1** are $J_1 = -4.60(2)$ cm^{-1}, $J_2 = +0.32(2)$ cm^{-1}, $J_3 = -1.10(1)$ cm^{-1}, and $g = 1.99$, with $R = 5.2 \times 10^{-5}$ (R being the agreement factor defined as $\sum[(\chi_M)_{obs} - (\chi_M)_{calc}]^2/\sum[(\chi_M)_{obs}]^2$). A common g value was assumed for Mn(II) and Mn(III) ions in the fit procedure. The computed curve for **1** (solid line in Figure 5) reproduces very well the magnetic data in the whole temperature range investigated. Some metric structural differences found among the Mn^{II}−Mn^{III} pathways lead us to separate them into two subgroups, one with Mn^{II}−Mn^{III} distances of 3.1−3.2 Å and Mn−O−Mn angles in the range of about 95−98°, and the other one with Mn^{II}−Mn^{III} distances of 3.3−3.5 Å and Mn−O−Mn angles in the range 98−113°. However, these structural differences proved to be unimportant, given that no significant improvement of the fit of the magnetic data of **1** was obtained through a spin Hamiltonian with four J parameters. Hence, to avoid overparametrization, all the Mn^{II}−Mn^{III} pathways were

dx.doi.org/10.1021/ic4016355 | Inorg. Chem. 2013, 52, 11934−11943

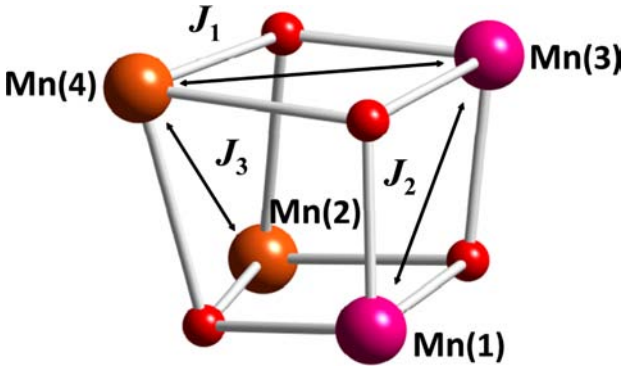

Figure 6. $[Mn^{II}_2Mn^{III}_2]$ core of **1** along with the exchange coupling pattern (see text). Color code: orange, pink, and red stand for manganese(II), manganese(III), and oxygen, respectively.

considered to be equal in the Hamiltonian of eq 1 by assuming only average structural parameters. Attempts to fit the experimental data, especially in the low temperature region through inclusion of both intercubane interactions and zfs gave very small values for these parameters and neither significantly modify the values of the intracubane magnetic couplings nor the quality of the fit.

It deserves to be pointed out that the synthesis and characterization of the first $Mn^{II}_2Mn^{III}_2$ cubane complex of formula $[Mn_4(L)_2(O)_2(CH_3CO_2)_2](ClO_4)_2{\cdot}2C_2H_5OH{\cdot}2H_2O$ (HL = 2,6-bis{*N*-(4-imidazol-yl-ethyl)iminomethyl}-4-methyl-phenol) was reported in 1995,[25] but its magnetic properties were only investigated from room temperature to that of the liquid nitrogen. As far as we know, the values of the magnetic couplings for **1** reported herein are the first ones which have been determined for the involved metal ions connected by alkoxo and carboxylato groups in a cubane core and, therefore, any comparison is precluded. Nevertheless, these values could roughly be compared with those of some similar fragments such as tetranuclear $Mn^{II}_2Mn^{III}_2$ (butterfly or rhombus core)[19−24] and Mn^{II}_4 (cubane core)[35] species with MnO_6 chromophores.

Focusing on the Mn^{III}−Mn^{III} and Mn^{II}−Mn^{II} magnetic interactions, one can see that in most of the Mn_4 complexes with a $Mn^{II}_2Mn^{III}_2$ rhombus core, the value of the Mn^{III}−O−Mn^{III} angle varies in the range about 97−103°. When the $Mn^{III}\cdots Mn^{III}$ distance is ≥ 3.1 Å, the magnitude of the magnetic coupling between Mn(III) ions, in such cases, is ferromagnetic, and its magnitude decreases with the increasing angle at the bridging oxygen,[24] indicating that orbital overlap (and then the antiferromagnetic contribution) is reinforced with the increase of the angle at the monatomic bridge. In this particular type of systems displaying a $Mn^{II}_2Mn^{III}_2$ rhombus-like core, when the Mn^{III}−O−Mn^{III} angle is about 103° and the $Mn^{III}\cdots Mn^{III}$ distance about 3.35 Å, the exchange coupling constant associated to the Mn^{III}−Mn^{III} interaction is always found to be ferromagnetic and varying from about +0.14 to +3.40 cm^{-1}.[24]

Therefore, the value of J_2 obtained for **1** (+0.32 cm^{-1}, with values for Mn^{III}−O−Mn^{III} and $Mn^{III}\cdots Mn^{III}$ of 102° and 3.35 Å, respectively) falls pretty well into this range. On the other hand, most of the reported Mn^{II}_4 cubane-type complexes show an anferromagnetic coupling between the Mn(II) ions.[35]

Because of the small Mn^{II}−O−Mn^{II} angles displayed in **1** (average value about 93.2°), the expected exchange coupling between Mn(II) metal ions is predicted to be weak either ferro- or antiferromagnetic. The weak antiferromagnetic coupling found for this pathway in **1** (J_3 = −1.1 cm^{-1}) agrees with this prediction. Finally, the obtained J_1 value (−4.6 cm^{-1}) is of the same sign and reasonably close to the exchange couplings obtained for Mn^{II}−Mn^{III} interactions in other complexes from the literature with metric structural parameters similar to those found for the Mn^{II}−Mn^{III} pathways in **1**.[36]

The magnetic properties of **2** under the form of both $\chi_M T$ and χ_M versus T plots (χ_M being the magnetic susceptibility per Cu^{II}_4 tetranuclear unit) are shown in Figure 7. $\chi_M T$ at 300 K is

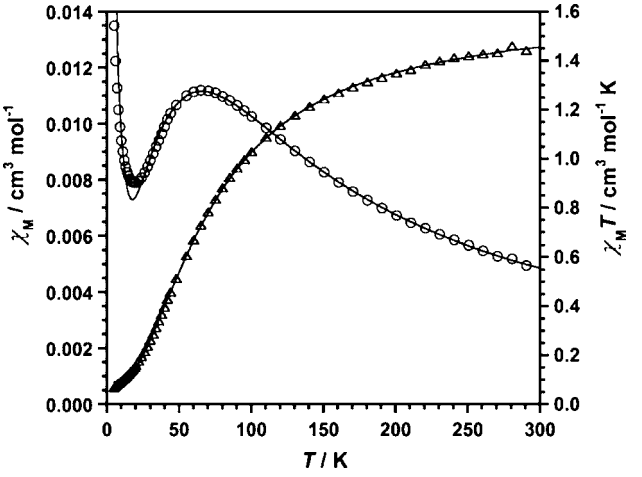

Figure 7. Thermal variation of χ_M (O) and $\chi_M T$ (Δ) for **2**. The solid lines are the best-fit curves (see text).

about 1.45 cm^3 mol^{-1} K, a value which is as expected for four uncoupled Cu(II) ions ($S_{Cu(II)}$ = 1/2). Upon cooling, $\chi_M T$ decreases very fast and tends to vanish practically at 1.9 K. A maximum of the magnetic susceptibility occurs in the χ_M vs T plot for **2** at 65.0 K. These features are characteristic of an overall antiferromagnetic coupling in **2** that leads to a S = 0 low-lying spin state. The increase of χ_M after the maximum at very low temperatures in the χ_M versus T plot is most likely because of a small percentage of paramagnetic impurities. In previous works dealing with Cu_4O_4 cubane-type structures, where the four O atoms generally belong to hydroxo,[37] alkoxo,[38] or phenoxo[39] bridges, two classifications of such systems have been proposed and used to correlate their structural features with magnetic behaviors. According to Mergehenn and Haase,[40] these compounds can be grouped into two types (I and II), depending on the length of the Cu−O bonds in the cubane moiety. Cu_4O_4 cubane complexes with four long Cu−O distances between two dinuclear subunits belong to type I, whereas those with long Cu−O distances within each dinuclear subunit belong to type II.

More recently, Alvarez and co-workers alternatively proposed to classify these systems according to the Cu···Cu distances instead,[26d,27] and divided this family into three different classes, namely, 2 + 4 (or equivalent to type I), 4 + 2 (Cu_4O_4 cubanes with four short and two long Cu···Cu distances, those with S_4 symmetry would be equivalent to type II), and 6 + 0 (those with six similar Cu···Cu distances), see Figure 8a. Having in mind these classifications, **2** falls into the category type I or 2 + 4, given that its two stacked dinuclear Cu_2O_2 subunits are linked by four long Cu−O bonds (Table 4).

Given the tetranuclear structure of **2** and the above features, we have analyzed the experimental magnetic data through the

dx.doi.org/10.1021/ic4016355 | *Inorg. Chem.* 2013, 52, 11934−11943

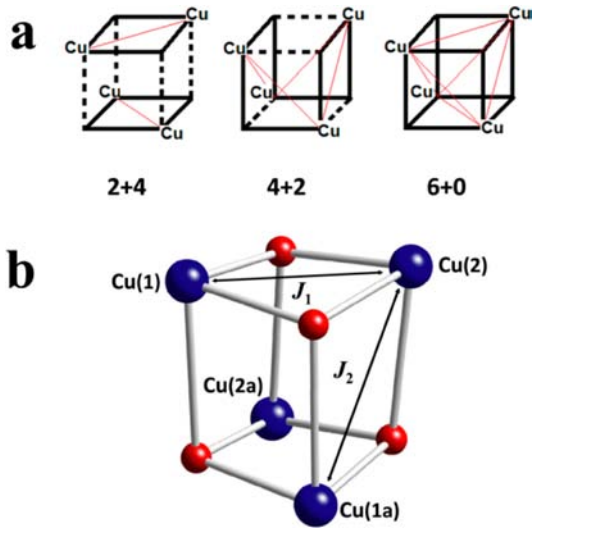

Figure 8. (a) Schematic drawing of the structural types of $[Cu_4O_4]$ cubane-type copper(II) complexes classified according to their short Cu···Cu distances (red lines). Short and long Cu−O bond lengths are indicated by black solid and broken lines, respectively. (b) A view of the $[Cu_4O_4]$ core of **2** with the exchange coupling pattern (see text).

theoretical expression for the magnetic susceptibility derived from the isotropic spin Hamiltonian of eq 2

$$\hat{H} = -J_1(\hat{S}_1\cdot\hat{S}_2 + \hat{S}_3\cdot\hat{S}_4) - J_2(\hat{S}_1 + \hat{S}_2)\cdot(\hat{S}_3 + \hat{S}_4) \quad (2)$$

where J_1 and J_2 are the intra- and interdinuclear exchange coupling constants between the local spin within the Cu_4O_4 cubane core (see Figure 8b). In addition, the θ and ρ parameters were included to account for intercubane magnetic interactions and paramagnetic impurities, respectively. Least-squares best-fit parameters are $J_1 = -58.1(3)$ cm^{-1}, $J_2 = +1.8(2)$ cm^{-1}, $g = 2.10$, $\theta = -0.03$ K, and $\rho = 2.7\%$ with $R = 1.4 \times 10^{-5}$ [R being the agreement factor defined as $\sum_i[(\chi_M)_{obs} - (\chi_M)_{calc}]^2/\sum_i[(\chi_M T)_{obs}]^2$]. As observed in Figure 7, the calculated curves for **2** (solid lines) match well the experimental magnetic data in the whole temperature range. The J_i values are in agreement with those from previously reported for 2 + 4 cubane-like copper(II) complexes.[37,38] The value of J_1 indicates that a relatively strong antiferromagnetic coupling occurs between the Cu(II) ions within each dinuclear Cu_2O_2 subunit of **2**, whereas a weak ferromagnetic coupling (J_2) accounts for the interaction between the two dinuclear subunits.

The value of $-J_1$ obtained for **2** is smaller than several earlier reported values for this parameter in alkoxo-bridged 2 + 4 Cu_4O_4 cubanes.[38] This fact is certainly attributed to the relatively small values of the Cu(1)−O−Cu(2) angles observed in **2** (av. value 96.7°) to be compared with those of the literature [mean value ca. 100° within the same Cu_2O_2 subunit].[38]

The signs of J_1 and J_2 obtained for **2** agree with previous Density Functional Theory (DFT) calculations performed on models of 2 + 4 systems.[26d,27] In such DFT studies, J_2 was found to be weakly ferromagnetic and practically independent of the geometry, whereas the value of J_1 resulted to be strongly dependent on the Cu−O−Cu angle and the substituent at the bridging oxygen atom. So that, in compounds with hydroxo-bridging ligands and small Cu−O−Cu bond angles J_1 should be ferromagnetic, but antiferromagnetic in alkoxo-bridged complexes, as observed in **2**.

A very nice agreement is also obtained for the correlation that exists between the so-called out-of-plane distortion of the substituent on the bridging oxygen atom (τ angle), the Cu−O−Cu angle, and the sign and magnitude of J. It is well-known that small values of the Cu−O−Cu angle are combined with the largest values of τ (av. value 42.2° for **2**), and these structures result in the weakest antiferromagnetic interactions.[27a]

To date, only one example of alkoxo-bridged 2 + 4 cubane that does not exhibit $S = 0$ ground state has been reported,[38d] its overall ferromagnetic coupling being associated with smaller Cu−O−Cu angles which vary in the range 89.8−94.4° [within the Cu_2O_2 subunits]. Anyway, the magnetic behavior of **2** is common for the majority of alkoxo-bridged tetranuclear copper(II) complexes displaying a 2 + 4 core structure.[27,38]

CONCLUSIONS

In summary, the use of the monodeprotonated pyridoxine (PN-H) [PN = 3-hydroxy-4,5-bis(hydroxymethyl)-2-methylpyridine] or Vitamin B_6 as ligand has provided two new tetranuclear $Mn^{II}_2Mn^{III}_2$ and Cu^{II}_4 cubane-type compounds of formula $[Mn_4(PN\text{-}H)_4(CH_3CO_2)_3Cl_2]Cl\cdot 2CH_3OH\cdot 2H_2O$ (**1**) and $[Cu_4(PN\text{-}H)_4Cl_2(H_2O)_2]Cl_2$ (**2**) which have been magneto-structurally investigated. In this experimental work the pyridoxine hydrochloride was used as the ligand source coupled to copper(II) or manganese(III) acetate salts aiming at inducing the formation of the monodeprotonated form (PN-H). This strategy has been successful, because in both compounds pyridoxine appears in its monodeprotonated form. Moreover, it is well-known that simple carboxylate ligands (like acetate) are used to preform small clusters that can further self-assemble upon the assistance of suitable organic ligands. This is the case of **1** where the acetate group also acts as ancillary ligand, most likely because of the greater overall charge on the cubane moiety, assisting the assembling of the Mn(II)/(III) metal ions in the cluster. The study of the magnetic properties of **1** and **2** shows that both compounds exhibit an overall antiferromagnetic behavior with coexistence of intracubane antiferro- and ferromagnetic interactions leading to a diamagnetic ground spin state. The J values for **1** are the first ones which have been determined for a tetranuclear $Mn_2^{II}Mn_2^{III}$ complex where metal ions are connected by alkoxo and carboxylato groups in a cubane core. This work is also the first magneto-structural study performed on pyridoxine-based complexes including **1**, an unusual example of tetranuclear mixed-valence $Mn_2^{II}Mn_2^{III}$ complex displaying a complete cubane core. Furthermore, the structural knowledge of **1** and **2** opens new gates envisaging the construction of low-dimensional polynuclear compounds based on bio-organic ligands.

ASSOCIATED CONTENT

Supporting Information

X-ray crystallographic files (CIF) for compounds **1** and **2** and SI file for more detailed crystal packing description of **1** and **2**. This material is available free of charge via the Internet at http://pubs.acs.org.

AUTHOR INFORMATION

Corresponding Authors

*E-mail: donatella.armentano@unical.it (D.A.).
*E-mail: F.Jose.Martinez@uv.es (J.M.-L.).

Notes

The authors declare no competing financial interest.

■ ACKNOWLEDGMENTS

Financial support from the Italian Ministero dell'Istruzione, dell'Università e della Ricerca Scientifica through the Centro di Eccellenza CEMIF.CAL (Grant CLAB01TYEF), the Spanish Ministerio de Ciencia e Innovación (Grant CTQ2010-15364) and the Consolider Ingenio in Molecular Nanoscience (Grant CSD2007-00010) is gratefully acknowledged.

■ REFERENCES

(1) (a) Yang, H.; Metera, K. L.; Sleiman, H. F. *Coord. Chem. Rev.* **2010**, *254*, 2403. (b) Singh, A.; Tolev, M.; Meng, M.; Klenin, K.; Plietzsch, O.; Schilling, C. I.; Muller, T.; Nieger, M.; Wenzel, S. W.; Richert, C. *Angew. Chem., Int. Ed.* **2011**, *50*, 3227. (c) Bandy, T. J.; Brewer, A.; Burns, J. R.; Marth, G.; Nguyen, T. N.; Stulz, E. *Chem. Soc. Rev.* **2011**, *40*, 138. (d) Duprey, J.-L. H. A.; Takezawa, Y.; Shionoya, M. *Angew. Chem., Int. Ed.* **2013**, *52*, 1212.

(2) (a) Smaldone, R. A.; Forgan, R. S.; Furukawa, H.; Gassensmith, J. J.; Slawin, A. M. Z.; Yaghi, O. M.; Stoddart, J. F. *Angew. Chem., Int. Ed.* **2010**, *49*, 46. (b) Imaz, I.; Rubio-Martínez, M.; An, J.; Solé-Font, I.; Rosi, N. L.; Maspoch, D. *Chem. Commun.* **2011**, *47*, 7287. (c) Liu, Y.-Q. Y.; Tang, Z. *Chem.—Eur. J.* **2012**, *18*, 4. (d) Zheng, H.-L.; Zhu, X.-X.; Guo, J.-Y.; Liu. *Solid State Sci.* **2013**, *18*, 42.

(3) (a) Armentano, D.; Mastropietro, T. F.; Julve, M.; Rossi, R.; Rossi, P.; De Munno, G. *J. Am. Chem. Soc.* **2007**, *129*, 2740. (b) Armentano, D.; Marino, N.; Mastropietro, T. F.; Martínez-Lillo, J.; Cano, J.; Julve, M.; Lloret, F.; De Munno, G. *Inorg. Chem.* **2008**, *47*, 10229. (c) Marino, N.; Armentano, D.; Mastropietro, T. F.; Julve, M.; Lloret, F.; De Munno, G. *Cryst. Growth Des.* **2010**, *10*, 1757.

(4) Acquaye, J. H. K. A.; Richardson, M. F. *Inorg. Chim. Acta* **1992**, *201*, 101.

(5) (a) Chaitanya Lakshmi, G.; Ananda, S.; Made Gowda, N. M. *Synth. React. Inorg., Met.-Org. Nano-Met. Chem.* **2009**, *39*, 434. (b) Chaitanya Lakshmi, G.; Ananda, S.; Made Gowda, N. M. *J. Chem. Chemical. Eng.* **2010**, *4*, 33. (c) Chaitanya Lakscmi, G.; Ananda, S.; Made Gowda, N. M. *Synth. React. Inorg., Met.-Org. Nano-Met. Chem.* **2011**, *41*, 1.

(6) (a) Kostakis, G. E.; Ako, A. M.; Powell, A. K. *Chem. Soc. Rev.* **2010**, *39*, 2238. (b) Brechin, E. K. *Chem Commun.* **2005**, 5141.

(7) Casas, J. S.; Castiñeiras, A.; Condori, F.; Couce, M. D.; Russo, U.; Sánchez, A.; Sordo, J.; Varela, J. M.; Vázquez-López, E. M. *J. Organomet. Chem.* **2004**, *689*, 620.

(8) Casas, J. S.; Castellano, E. E.; Condori, F.; Couce, M. D.; Sánchez, A.; Sordo, J.; Varela, J. M.; Zuckerman-Schpector, J. *J. Chem. Soc., Dalton Trans.* **1997**, 4421.

(9) Mathews, I. I.; Manohar, H. *J. Chem. Soc., Dalton Trans.* **1991**, 2139.

(10) Sabirov, V. Kh.; Batsanov, A. S.; Struchkov, Y. T.; Azizov, M. A.; Shabilalov, A. A.; Pulatov, A. S. *Koord. Khim. (Russ.), Coord. Chem.* **1984**, *10*, 275.

(11) Chamayou, A. C.; Neelakantan, M. A.; Thalamuthu, S.; Janiak, C. *Inorg. Chim. Acta* **2011**, *365*, 447.

(12) Bonfada, E.; de Oliveira, G. M.; Back, D. F.; Lang, E. S. *Z. Anorg. Allg. Chem.* **2005**, *631*, 878.

(13) Rao, S. P. S.; Varughese, K. I.; Manohar, H. *Inorg. Chem.* **1986**, *25*, 734.

(14) (a) Sabirov, V. K.; Struchkov, Y. T.; Batsanov, A. S.; Azizov, M. A. *Koord. Khim. (Russ.) Coord. Chem.* **1982**, *8*, 1623. (b) Makhyoun, M. A.; Al-Salem, N. A.; El-Ezaby, M. S. *Inorg. Chim. Acta* **1986**, *123*, 117. (c) Dey, S.; Banerjee, P.; Gangopadhyay, S.; Vojtisek, P. *Transition Met. Chem.* **2003**, *28*, 765.

(15) Sabirov, V. K.; Batsanov, A. S.; Struchkov, Y. T.; Azizov, M. A. *Koord. Khim. (Russ.) Coord. Chem.* **1983**, *9*, 1701.

(16) (a) Furmanova, N. G.; Berdalieva, Zh. I.; Chernaya, T. S. *Crystallogr. Rep.* **2009**, *54*, 228. (b) Furmanova, N. G.; Verin, I. A.; Shyityeva, N.; Sulaimankulov, K. S.; Berdalieva, Zh.; Resnyanskii, V. F.; Duishenbaeva, A. T. *Crystallogr. Rep.* **2011**, *56*, 1033.

(17) (a) Rao, P. V.; Holm, R. H. *Chem. Rev.* **2004**, *104*, 527. (b) Mullins, C. J.; Pecoraro, V. L. *Coord. Chem. Rev.* **2008**, *252*, 416. (c) Barber, J.; Murray, J. W. *Coord. Chem. Rev.* **2008**, *252*, 433.

(18) (a) Gatteschi, D.; Sessoli, R. *Angew. Chem., Int. Ed.* **2003**, *42*, 268. (b) Bircher, R.; Chaboussant, G.; Dobe, C.; Gudel, H. U.; Ochsenbein, S. T.; Sieber, A.; Waldmann, O. *Adv. Funct. Mater.* **2006**, *16*, 209. (c) Bagai, R.; Christou, G. *Chem. Soc. Rev.* **2009**, *38*, 1011 and references cited therein.

(19) (a) McCrea, J.; McKee, V.; Metcalfe, T.; Tandon, S. S.; Wikaira, J. *Inorg. Chim. Acta* **2000**, *297*, 220. (b) Sanudo, E. C.; Grillo, V. A.; Knapp, M. J.; Bollinger, J. C.; Huffman, J. C.; Hendrickson, D. N.; Christou, G. *Inorg. Chem.* **2002**, *41*, 2441. (c) Milios, C. J.; Raptopoulou, C. P.; Terzis, A.; Vicente, R.; Escuer, A.; Perlepes, S. P. *Inorg. Chem. Commun.* **2003**, *6*, 1056. (d) Stamatatos, T. C.; Adam, R.; Raptopoulou, C. P.; Psycharis, V.; Ballesteros, R.; Abarca, B.; Perlepes, S. P.; Boudalis, A. K. *Inorg. Chem. Commun.* **2012**, *15*, 73.

(20) Price, D. J.; Batten, S. R.; Berry, K. J.; Moubaraki, B.; Murray, K. S. *Polyhedron* **2003**, *22*, 165.

(21) (a) Brechin, E. K.; Yoo, J.; Nakano, M.; Huffman, J. C.; Hendrickson, D. N.; Christou, G. *Chem.Commun.* **1999**, 783. (b) Yoo, J.; Brechin, E. K.; Yamaguchi, A.; Nakano, M.; Huffman, J. C.; Maniero, A. L.; Brunel, L. C.; Awaga, K.; Ishimoto, H.; Christou, G.; Hendrickson, D. N. *Inorg. Chem.* **2000**, *39*, 3615. (c) Yoo, J.; Yamaguchi, A.; Nakano, M.; Krzystek, J.; Streib, W. E.; Brunel, L.-C.; Ishimoto, H.; Christou, G.; Hendrickson, D. N. *Inorg.Chem.* **2001**, *40*, 4604.

(22) Yang, C. I.; Lee, G. H.; Wur, C. S.; Lin, J. G.; Tsai, H. L. *Polyhedron* **2005**, *24*, 2215.

(23) Shao, C.-Y.; Zhu, L.-L.; Yang, P.-P. *Z. Anorg. Allg. Chem.* **2012**, *638*, 1307.

(24) (a) Vincent, J. B.; Christmas, C.; Chang, H.-R.; Li, Q.; Boyd, P.; Huffman, J. C.; Hendrickson, D. N.; Christou, G. *J. Am. Chem. Soc.* **1989**, *111*, 2086. (b) Thorp, H. H.; Sameski, J. E.; Kulawiec, R. J.; Brudvig, G. W.; Crabtree, R. H.; Papaefthymiou, G. C. *Inorg. Chem.* **1991**, *30*, 1153. (c) Sañudo, E. C.; Grillo, V. A.; Yoo, J.; Huffman, J. C.; Bollinger, J. C.; Hendrickson, D. N.; Christou, G. *Polyhedron* **2001**, *20*, 1269. (d) Yang, E. C.; Harden, N.; Wernsdorfer, W.; Zakhrov, L.; Brechin, E. K.; Rheingold, A. L.; Christou, G.; Hendrickson, D. N. *Polyhedron* **2003**, *22*, 1857. (e) Wittick, L. M.; Murray, K. S.; Moubaraki, B.; Batten, S. R.; Spiccia, L.; Berry, K. *Dalton Trans.* **2004**, 1003. (f) Miyasaka, H.; Nakata, K.; Sugiuara, K.-I.; Yamashita, M.; Clérac, R. *Angew. Chem., Int. Ed.* **2004**, *43*, 707. (g) Lecren, L.; Wernsdorfer, W.; Li, Y.-G.; Roubeau, O.; Miyasaka, H.; Clérac, R. *J. Am. Chem. Soc.* **2005**, *127*, 11311. (h) Lecren, L.; Roubeau, O.; Coulon, C.; Li, Y.-G.; Le Goff, X. F.; Wernsdorfer, W.; Miyasaka, H.; Clérac, R. *J. Am. Chem. Soc.* **2005**, *127*, 17353. (i) Foguet-Albiol, D.; O'Brien, T. A.; Wernsdorfer, W.; Moulton, B.; Zaworotko, M. J.; Abboud, K. A.; Christou, G. *Angew. Chem., Int. Ed.* **2005**, *44*, 897. (j) Yoo, J.; Wernsdorfer, W.; Yang, E.-C.; Nakano, M.; Rheingold, A. L.; Hendrickson, D. N. *Inorg. Chem.* **2005**, *44*, 3377. (k) Lecren, L.; Li, Y.-G.; Wernsdorfer, W.; Roubeau, O.; Miyasaka, H.; Clérac, R. *Inorg. Chem. Commun.* **2005**, *8*, 626. (l) Ako, A. M.; Mereacre, V.; Hewitt, I. J.; Clerac, R.; Lecren, L.; Anson, C. E.; Powell, A. K. *J. Mater. Chem.* **2006**, *16*, 2579. (m) Miyasaka, H.; Nakata, K.; Lecren, L.; Coulon, C.; Nakazawa, Y.; Fujisaki, T.; Sugiura, K.; Yamashita, M.; Clérac, R. *J. Am. Chem. Soc.* **2006**, *128*, 3770. (n) Hiraga, H.; Miyasaka, H.; Nakata, K.; Kajiwara, T.; Takaishi, S.; Oshima, Y.; Nojiri, H.; Yamashita, M. *Inorg. Chem.* **2007**, *46*, 9661. (o) Stamatatos, T. C.; Poole, K. M.; Abboud, K. A.; Wernsdorfer, W.; O'Brien, T. A.; Christou, G. *Inorg. Chem.* **2008**, *47*, 5006. (p) Baca, S. G.; Malaestean, I. L.; Keene, T. D.; Adams, H.; Ward, M. D.; Hauser, J.; Neels, A.; Decurtins, S. *Inorg. Chem.* **2008**, *47*, 11108. (q) Lecren, L.; Roubeau, O.; Li, Y.-G.; Le Goff, X. F.; Miyasaka, H.; Richard, F.; Wernsdorfer, W.; Coulona, C.; Clérac, R. *Dalton Trans.* **2008**, 755. (r) Jerzykiewicz, L. B.; Utko, J.; Duczmal, M.; Starynowicz, P.; Sobota, P. *Eur. J. Inorg. Chem.* **2010**, 4492.

(25) Mikuriya, M.; Hashimoto, Y.; Kawamori, A. *Chem. Lett.* **1995**, 1095.

(26) See for example: (a) Oshio, H.; Saito, Y.; Ito, T. *Angew. Chem., Int. Ed.* **1997**, *36*, 2673. (b) Mukherjee, A.; Raghunathan, R.; Saha, M. K.; Nethaji, M.; Ramasesha, S.; Chakravarty, A. R. *Chem.—Eur. J.* **2005**, *11*, 3087. (c) Lopez, N.; Vos, T. E.; Arif, A. M.; Shum, W. W.; Noveron, J. C.; Miller, J. S. *Inorg. Chem.* **2006**, *45*, 4325. (d) Xie, Y.; Ni, J.; Zheng, F.; Cui, Y.; Wang, Q.; Ng, S. W.; Zhu, W. *Cryst. Growth Des.* **2009**, *9*, 118.
(27) (a) Ruiz, E.; Rodríguez-Fortea, A.; Alemany, P.; Alvarez, S.; Cano, J. *J. Am. Chem. Soc.* **1997**, *119*, 1297. (b) Ruiz, E.; Rodríguez-Fortea, A.; Alemany, P.; Alvarez, S. *Polyhedron* **2001**, *20*, 1323. (c) Tercero, J.; Ruiz, E.; Alvarez, S.; Rodríguez-Fortea, A.; Alemany, P. *J. Mater. Chem.* **2006**, *16*, 2729.
(28) Sheldrick, G. M. *SADABS Program for Absorption Correction*, version 2.10; Bruker Analytical X-ray Systems: Madison, WI, 2003.
(29) (a) Sheldrick, G. M. *Acta Crystallogr.* **2008**, *A64*, 112. (b) *SHELXTL*; Bruker Analytical X-ray Instruments: Madison, WI, 1998.
(30) Müller, P. *Crystallogr. Rev.* **2009**, *15*, 57−83.
(31) (a) Spek, A. L. *Acta Crystallogr.* **1990**, *A46*, C34. (b) Van der Sluis, P.; Spek, A. L. *Acta Crystallogr.* **1990**, *A46*, 194.
(32) Brandenburg, K.; Putz, H.*DIAMOND*, 2.1d; Crystal Impact GbR: Bonn, Germany, 2000.
(33) (a) Brown, I. D.; Altermatt, D. *Acta Crystallogr., Sect. B: Struct. Sci.* **1985**, *41*, 244. (b) Liu, W.; Thorp, H. H. *Inorg. Chem.* **1993**, *32*, 4102.
(34) Cano, J. *VMPAG package*; University of Valencia: Valencia, Spain, 2003.
(35) (a) Brooker, S.; McKee, V.; Shepard, W. B.; Pannell, L. K. *J. Chem. Soc., Dalton Trans.* **1987**, 2555. (b) Aussoleil, J.; Cassoux, P.; de Loth, P.; Tuchagues, J.-P. *Inorg. Chem.* **1989**, *28*, 3051. (c) Murray, K. S. *Adv. Inorg. Chem.* **1995**, *43*, 261. (d) Brooker, S.; McKee, V.; Metcalfe, T. *Inorg. Chim. Acta* **1996**, *246*, 171. (e) Pence, L. E.; Caneschi, A.; Lippard, S. J. *Inorg. Chem.* **1996**, *35*, 3069. (f) Tong, M.-L.; Zheng, S.-L.; Shi, J.-X.; Tong, Y.-X.; Lee, H. K.; Chen, X.-M. *J. Chem. Soc., Dalton Trans.* **2002**, 1727. (g) Shiga, T.; Oshio, H. *Sci. Tech. Adv. Mater.* **2005**, *6*, 565. (h) Papaefstathiou, G. S.; Escuer, A.; Mautner, F. A.; Raptopoulou, C. P.; Terzis, A.; Perlepes, S. P.; Vicente, R. *Eur. J. Inorg. Chem.* **2005**, 879. (i) Shiga, T.; Oshio, H. *Sci. Technol. Mater.* **2005**, *6*, 565. (j) Hudson, T. A.; Berry, K. J.; Moubaraki, B.; Murray, K. S.; Robson, B. *Inorg. Chem.* **2006**, *45*, 3549. (k) Stoumpos, C. C.; Gass, I. A.; Milios, C. J.; Kefalloniti, E.; Raptopoulou, C. P.; Terzis, A.; Lalioti, N.; Brechin, E. K.; Perlepes, S. P. *Inorg. Chem. Commun.* **2008**, *11*, 196. (l) Stoumpos, C. C.; Gass, I. A.; Milios, C. J.; Lalioti, N.; Terzis, A.; Aromi, G.; Teat, S. J.; Brechin, E. K.; Perlepes, S. P. *Dalton Trans.* **2009**, 307.
(36) Saha, A.; Abboud, K. A.; Christou, G. *Inorg.Chem.* **2011**, *50*, 12774 and references therein cited.
(37) (a) Sletten, J.; Sorensen, A.; Julve, M.; Journaux, Y. *Inorg. Chem.* **1990**, *29*, 5054. (b) Eberhardt, J. K.; Glaser, T.; Hoffmann, R. D.; Fröhlich, R.; Würsthwein, E. U. *Eur. J. Inorg. Chem.* **2005**, 1175.
(38) (a) Fallon, G. D.; Moubaraki, B.; Murray, K. S.; Van der Bergen, A. M.; West, B. O. *Polyhedron* **1993**, *12*, 1989. (b) Wang, S.; Zheng, J.-C.; Hall, J. R.; Thompson, L. K. *Polyhedron* **1994**, *13*, 1039. (c) Xie, Y.; Bu, W.; Xu, X.; Jiang, H.; Liu, Q.; Xue, Y.; Fan, Y. *Inorg. Chem. Commun.* **2001**, *4*, 558. (d) Burkhardt, A.; Spielberg, E. T.; Görls, H.; Plass, W. *Inorg. Chem.* **2008**, *47*, 2485.
(39) (a) Lopes, C.; M. Håkansson, M.; S. Jagner, S. *Inorg. Chim. Acta* **1997**, *254*, 361. (b) Yamashita, H.; Koikswa, M.; Tokii, T. *Mol. Cryst. Liq. Cryst.* **2000**, *342*, 63. (c) Gustafsson, B.; Håkansson, M.; Westman, G.; Jagner, S. *J. Organomet. Chem.* **2002**, *649*, 204. (d) Chakraborty, J.; Thakurta, S.; Pilet, G.; Luneau, D.; Mitra, S. *Polyhedron* **2009**, *28*, 819.
(40) (a) Mergehenn, R.; Haase, W. *Acta Crystallogr., Sect. B* **1977**, *33*, 1877. (b) Mergehenn, R.; Merz, L.; Haase, W. *J. Chem. Soc., Dalton Trans.* **1980**, 1703.